PCCP

PAPER

Cite this: *Phys. Chem. Chem. Phys.*, 2016, **18**, 24922

Encapsulation of spherical nanoparticles by colloidal dimers

Gianmarco Munaò,*[a] Dino Costa,[a] Santi Prestipino[ab] and Carlo Caccamo[a]

Received 6th July 2016,
Accepted 8th August 2016

DOI: 10.1039/c6cp04704a

www.rsc.org/pccp

We study by Monte Carlo simulation the coating process of colloidal dimers onto spherical nanoparticles. To this end we investigate a simplified mixture of hard spheres (the guest particles) and hard dimers formed by two tangent spheres of different sizes (the encapsulating agents) in an implicit-solvent representation; in our scheme, the range of effective interactions between the smaller particle in a dimer and a guest sphere depends on their relative size. By tuning the size and concentration of guests, under overall dilute conditions a rich phase behavior emerges: for small sizes and/or low concentrations, the preferred arrangement is compact aggregates (capsules) of variable sizes, where one or few guest particles are coated with dimers; for larger sizes and moderate guest concentrations, other scenarios are realized, including equilibrium separation between a guest-rich and a guest-poor phase. Our results serve as a framework for a more systematic investigation of self-assembled structures of functionalized dimers capable of encapsulating target particles, like for instance bioactive substances in a colloidal dispersion.

I Introduction

In the last few years, the mechanism of the formation of a coating layer (nanocapsule) around a target species has been capturing large fundamental and technological interest; to quote a few applications, encapsulation is essential in the pharmaceutical field, where it plays an important role in drug delivery in the human body[1,2] or as a means to protect proteins, peptides, and DNA from coming into contact with the external environment;[3–6] in the food industry, encapsulation may be used to preserve the quality of nutraceuticals.[7–9] The main virtue of encapsulation is the temporary "protection" that the external shell provides to an enclosed guest object; once the capsule has formed, the controlled release of the guest will take place under prescribed conditions.

In essence, encapsulation can be implemented by two different approaches: in the first case, one studies the interaction between a predefined nanocapsule shell, composed of a fixed number of particles, and the target. The advantage of this approach is that the capsule structure is given at the outset so that the investigation can be focused on the encapsulation process itself. Applications of this method include the analysis of the permeability of encapsulating agents[10] and the investigation of their mechanical and geometrical properties.[11] In a different scheme, the encapsulating structures are not given in advance, but they arise spontaneously through a self-assembly process. Within this framework, the possibility to control the size and the shape of the aggregated structures, as well as to properly fix the potential parameters, is of foremost importance. In particular, the self-assembling properties of amphiphilic molecules, lipids, and block copolymers are very promising.[2,12,13] Very recently, protein-like copolymers have also been proposed as coating agents for small-molecule solutes.[14]

Among the wide range of particles that may be used for encapsulation, colloidal dimers deserve special interest, as witnessed by the considerable number of experimental[15–19] and numerical studies[20–22] that were devoted to the investigation of the influence of microscopic interactions on the macroscopic behavior of these systems. The reason for such interest stems from the opportunity, offered by modern experimental protocols, to engineer the molecular geometry and the interaction potential of dimers, in order to induce a variety of phase behaviors.[23,24] In particular, if one of the particles forming the dimer is solvophilic while the other is solvophobic, we obtain "Janus dimers",[25,26] *i.e.* colloids representing the molecular analogs of Janus spheres.[27,28] The latter have been widely investigated, since they give rise to a large variety of supramolecular aggregates.[29–32] A recently developed model of Janus ellipsoids[33–35] has provided a clear demonstration of the potentialities of such particles as encapsulating agents. Janus dimers, like their "atomic" counterparts, are also able to form complex self-assembled structures such as micelles,[36] vesicles,[37] and bilayers.[38] The possibility to form such diverse superstructures makes Janus dimers natural candidates for investigating the formation of encapsulating shells around guest particles. Moreover, dimers are more ductile than spheres, owing to the greater freedom allowed by the possibility to separately adjust the relative distance

[a] *Dipartimento di Scienze Matematiche e Informatiche, Scienze Fisiche e Scienze della Terra, Universitá degli Studi di Messina, Viale F. Stagno d'Alcontres 31, 98166 Messina, Italy. E-mail: gmunao@unime.it*
[b] *CNR – Istituto per i Processi Chimico-Fisici, Viale F. Stagno d'Alcontres 37, 98158 Messina, Italy*

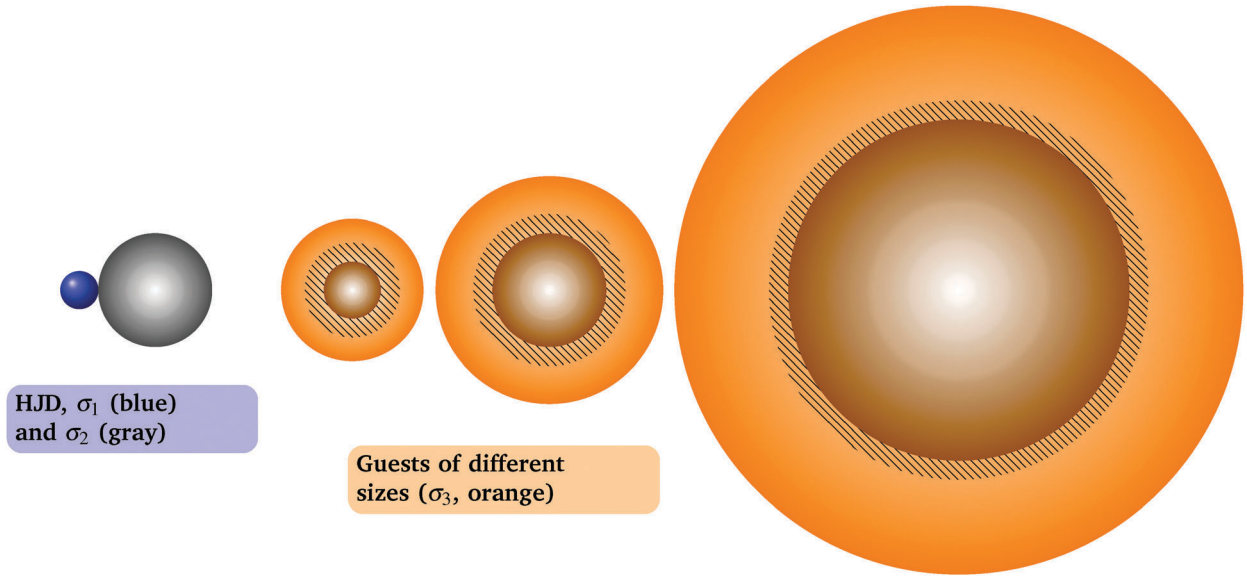

Fig. 1 The model mixture studied in this work. HJD (hard-sphere dimer on the left, with size ratio σ_1/σ_2 = 1/3) and guest particles of three different diameters (hard spheres on the right, with σ_3/σ_2 = 0.5, 1.0 and 3.0). Shaded areas and halos around each guest have a width of $\sigma_1/2$ and $\lambda\sigma_{13} - \sigma_1/2$, respectively (see eqn (1)).

and size of the monomers. In this work we investigate by Monte Carlo simulation the spontaneous formation (*i.e.* through self-assembly) of coating layers around hard spherical particles (guests), with Janus dimers acting as encapsulating agents. Following earlier studies,[24,36] Janus dimers are modeled by two tangent hard spheres of different sizes, the smaller one further interacting with guests through a square-well attraction. This basic model mimics, in an implicit-solvent description, a colloidal solution formed by the solvent, a guest species, and an amphiphilic dimer with a solvophobic smaller monomer. Our conditions are descriptive of a mixture where the cross-attraction between dimers and guest particles is much stronger than the attraction between like particles, thus making the formation of capsules to be preferred over the gathering together of dimers or guests only. Upon varying the size and the concentration of guest particles, we will show that such Janus dimers are able to spontaneously assemble around guests, provided that suitable thermodynamic conditions are met.

This paper is organized as follows. In Section II we describe our model and the simulation technique. The results are presented and discussed in Section III. Concluding remarks and perspectives follow in Section IV.

II Models and methods

The binary mixture studied in this work is schematically drawn in Fig. 1: a dimer is formed by a pair of tangent hard spheres with different core diameters, σ_1 and σ_2 (heteronuclear Janus dimers, HJDs; we henceforth assume $\sigma_1 = \sigma_2/3$). Guest particles are modeled as hard spheres of diameter σ_3, with the size ratio σ_3/σ_2 alternately taking the values 0.5, 1.0 or 3.0. All interactions are given by excluded volume effects, modeled as hard-sphere potentials with additive diameters $\sigma_{ij} = (\sigma_i + \sigma_j)/2$, plus an additional square-well (SW) attraction exclusively acting between the smaller site of a HJD (site 1) and a guest sphere (particle 3), in the form:

$$\phi_{sw}(r_{13}) = \begin{cases} \infty & \text{if} \quad r_{13} < \sigma_{13} \\ -\varepsilon & \text{if} \quad \sigma_{13} \leq r_{13} < (1+\lambda)\sigma_{13} \\ 0 & \text{otherwise,} \end{cases} \qquad (1)$$

where r_{13} is the interparticle separation between the centers of 1 and 3 (see Fig. 1). Here and elsewhere, by "site" we indicate the center of a monomer belonging to a HJD. Note that the range of ϕ_{sw} scales with σ_{13}, which is tantamount to assuming that the 1–3 attraction is rooted in the properties of the guest particles themselves rather than in the intermediation effect of the solvent. We also avoided introducing 1–1 and 3–3 interactions other than excluded-volume ones with the idea that the 1–3 interaction is much stronger. Clearly, this keeps to a minimum the number of parameters in our model. In all calculations we fixed λ = 0.5. In the following, σ_2 and ε are, respectively, taken as units of length and energy, with the reduced temperature defined as $T^* = k_B T/\varepsilon$ (k_B being the Boltzmann constant). The values of σ_1 and λ were so chosen that the interaction between a HJD and a guest particle does not result in such large steric effects as to hinder the encapsulation process. Moreover, the chosen λ allows us to observe the development of self-aggregated structures already for T^* = 0.15, which avoided us the demanding task to perform simulations for too low temperatures, where the equilibration of dimers may require extremely long times.[23]

We have determined the thermodynamic and structural properties of the mixture, as well as the geometry of the self-assembled structures, by means of Metropolis Monte Carlo (MC) simulations in the canonical ensemble, on two different samples made up of N = 1372 and 5400 molecules in total,

Table 1 Sizes and packing fractions of guests for $\chi \leq 20\%$: η_{guest} and η_{HJD}, respectively, concern guests and dimers, while $\eta = \eta_{guest} + \eta_{HJD}$. For samples of 1372 and 5400 molecules we have used different box edges (L_{box}/σ_2 = 30.16 and 47.62, respectively), so as to have the same reduced density $\rho{\sigma_2}^3 = 0.05$ in both cases

	χ = 1%			χ = 10%			χ = 20%		
σ_3/σ_2	η	η_{guest}	η_{HJD}	η	η_{guest}	η_{HJD}	η	η_{guest}	η_{HJD}
0.5	0.02683	3×10^{-5}	0.02680	0.0247	3×10^{-4}	0.0244	0.0223	6×10^{-4}	0.0217
1.0	0.0270	2×10^{-4}	0.0268	0.027	0.003	0.024	0.027	0.005	0.022
3.0	0.034	0.007	0.027	0.095	0.071	0.024	0.163	0.141	0.022

enclosed in a cubic box of volume V with periodic boundary conditions. All simulations have been carried out for a fixed reduced density $\rho^* = N{\sigma_2}^3/V = 0.05$. Calling N_{HJD} and $N_{guest} \equiv N - N_{HJD}$ the number of HJD molecules and guests, respectively, the concentration of the latter particles is $\chi \equiv N_{guest}/N$. We have considered three χ values (1%, 10%, and 20%), so as to perform investigations over a relatively wide range of sizes and concentrations of the guests. In particular, the number of guest particles is lower than the number of HJDs in order to favor encapsulation. We have also performed a small number of simulations in the opposite regime of very high concentrations of guests (χ = 90% and 95%), with the exclusive aim of comparing the local structure of the present system with that of pure hard spheres. In Table 1 we report packing-fraction data for the guest sizes and concentrations more extensively investigated in this work. For any state point we have first performed 5×10^5 MC steps per particle (cycles) in order to equilibrate the system, then computing statistical averages over the next million cycles. For the lowest temperatures ($T^* \leq 0.15$), we have employed up to five million cycles in order to ensure a proper equilibration even under such conditions. An equal number of cycles has been generated in the production stage. We have examined self-assembled structures and phase behaviors through bond distributions, radial distribution functions and visual inspection of the system configuration.

III Results

In our scheme, a bond is formed between one dimer and one guest if the distance between the guest sphere and the attracting site of the HJD falls in the range $\sigma_{13} \leq r_{13} \leq \sigma_{13}(1 + \lambda)$. On this basis we make a preliminary assessment of the coating properties of our model. Since the strength of 1–3 attraction is constant over this interval, the most favorite bond length is $R_{max} = \sigma_{13}(1 + \lambda)$, as the entropy is expected to increase with the radius of the coating shell. In this case, sites 2 form a spherical layer, centered on the guest particle, with radius $R_C = \sigma_{12} + R_{max} = 11/12 + (3/4)\sigma_3$. The densest allocation of sites 2 in the external shell occurs when they are tangent to each other (a goal which is obviously hampered by steric effects). The area occupied by each site 2 in the layer is $A_\sigma \simeq {\sigma_2}^2 = 1$; denoting N_{max} the maximum number of dimers around the guest sphere, we have $4\pi{R_C}^2 = N_{max}A_\sigma$, that is $N_{max} = 4\pi[11/12 + (3/4)\sigma_3]^2$. In Table 2 we compare N_{max} with the results, N_{sim}, of a series of MC simulations performed with N = 1372 at low temperature (T^* = 0.05), under conditions of infinite dilution corresponding to only one guest in a fluid of HJDs: we see that both N_{max} and N_{sim} quickly increase with σ_3, following an almost parabolic trend which is consistent with the corresponding increase of the guest surface. The agreement between N_{max} and N_{sim} improves upon increasing σ_3, while N_{sim} always turns to be smaller than N_{max}, suggesting that few dimers are also present inside the putative diameter of the capsule. Indeed, while estimating the number of sites 2 in the outer shell, we have neglected the mutual hindrance between the dimers; moreover, the energy can further be lowered by putting dimers in the interior of the capsule. In Fig. 2, we show a number of capsules formed for different σ_3 values: as is clear, the dimers are distributed at various distances from the center of the capsule; moreover, the coating shell exhibits a small, almost negligible porosity. If $\sigma_3/\sigma_2 \gg 1$ and the temperature is low enough, we expect a similarity of behavior to the case of hard disks embedded on a spherical surface.[39–41] In the latter model we know that the (triangular) crystal order is frustrated by geometry, which induces point defects (disclinations) in the system in quite definite proportions. The same coordination defects are seen in the coating layer of capsules (see Fig. 2c).

Table 2 Number of coating dimers for the case of a single guest of various sizes, according to theory (N_{max}) and simulation (N_{sim})

σ_3/σ_2	0.5	1	3
N_{max}	21	35	125
N_{sim}	14	26	122

In the rest of this section, we shall initially focus on relatively large guest particles, $\sigma_3 = 3\sigma_2$, moving later to guests of size comparable to σ_2 ($\sigma_3 = \sigma_2/2$ and $\sigma_3 = \sigma_2$). We have first carried out simulations for a low guest concentration, χ = 1%, and a number of temperatures between 0.15 and 0.30. This is the only case where we have employed a sample of N = 5400 particles, which ensures enough guest particles to make a reliable estimate of their statistical properties. Microscopic, structural, and thermodynamic properties for this case are reported in Fig. 3. The formation of capsules is evident in the distribution of the relative distance between the site 1 of a HJD and a guest sphere, as expressed by the radial distribution function (RDF) $g_{13}(r)$, plotted in panel (a). There we see that $g_{13}(r)$ drops to nearly zero for $r/\sigma_2 \approx 2.5$, corresponding to the width of the SW attraction, $(1 + \lambda)\sigma_{13}$; further beyond a shallow secondary peak, $g_{13}(r)$ practically attains the ideal-gas value. Comparing this case with the single-guest case of Table 2, we observe a reduction in the average number of coating dimers, as can be appreciated by the probability distribution of the

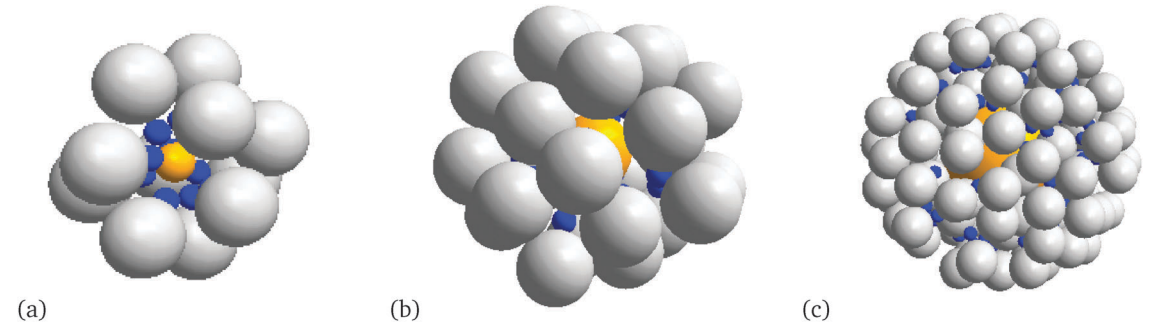

Fig. 2 Typical capsule structures resulting from the simulation of mixtures of the HJD and a single guest (for $T^* = 0.05$), with sizes $\sigma_3 = \sigma_2/2$ (a), σ_2 (b), and $3\sigma_2$ (c).

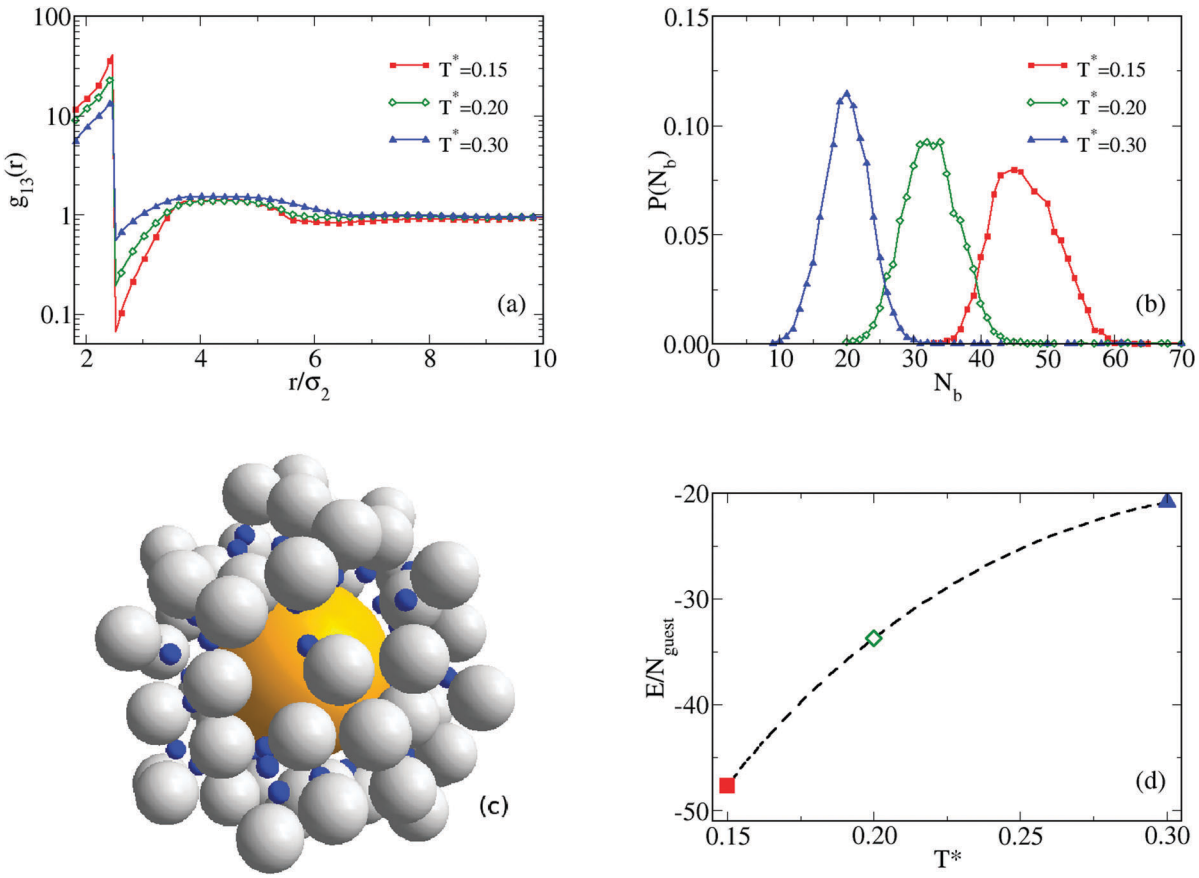

Fig. 3 Structure and thermodynamics of a mixture of HJDs and guest particles with $\sigma_3 = 3\sigma_2$ and $\chi = 1\%$: (a) $g_{13}(r)$ plotted on a semilogarithmic scale for a number of temperatures and (b) corresponding probability distributions of bonds $P(N_b)$; (c) structure of a typical capsule for $T^* = 0.15$ and (d) internal energy of the fluid.

average number N_b of bonds per guest, $P(N_b)$, reported in Fig. 3b: for $T^* = 0.15$, guest particles can bind from 35 to 60 dimers, with a most probable value of ≈ 47. The effect of heating on reducing the efficiency of encapsulation is evident in the same Fig. 3b: the number of dimers in the coating shell drops to ≈ 20 when the temperature is increased to $T^* = 0.30$. A typical snapshot of the capsule structure is shown in Fig. 3c: the coating layer is clearly less compact than in Fig. 2c (the pores are larger), but still well defined. Finally, we show in Fig. 3d the behavior of the internal energy per guest particle, E/N_{guest}. This quantity corresponds (in absolute value) to the average number of bonds formed by HJDs with guest particles; indeed, the value of E/N_{guest} is consistent with the probability distribution of Fig. 3b. As expected, the internal energy systematically increases with increasing temperature.

If we look at the amount of order in the spatial distribution of guests – as described by the $g_{33}(r)$ function of Fig. 4a – we notice a remarkably strong correlation between the guest positions over a narrow range of distances near contact. Upon heating, the contact value of $g_{33}(r)$ decreases and the function broadens up to a distance of $r \simeq 4\sigma_2$, signalling that several guest particles are sharing a common coating shell, with the HJD

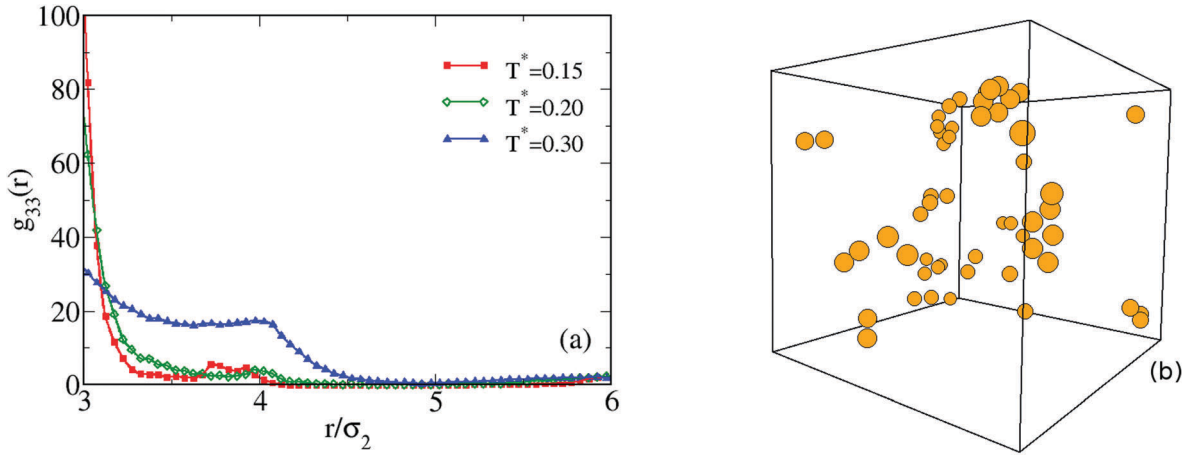

Fig. 4 Mixture of HJDs and guests with $\sigma_3 = 3\sigma_2$ and $\chi = 1\%$: (a) $g_{33}(r)$ for various temperatures and (b) a microscopic configuration for $T^* = 0.30$, where only guest particles are shown.

acting as a "glue" between them. The tendency of guest particles to aggregate is also apparent in the snapshot of Fig. 4b, where the HJDs have been removed for clarity: a small fraction of guests are isolated, and hence enclosed within capsules with only one sphere inside; but we also observe guest pairs, as well as more complex clusters, indicating multiple encapsulation. We underline that the formation of guest aggregates provides another explanation, in addition to heating, for the observed reduction in the average number of bonded dimers per guest with respect to the infinite-dilution case.

We now consider the effect of increasing the concentration of guests for fixed $\sigma_3 = 3\sigma_2$. The results for $\chi = 20\%$ point to a scenario different from encapsulation (see Fig. 5): as can be seen in the snapshot in panel (a), relative to $T^* = 0.30$, all guests

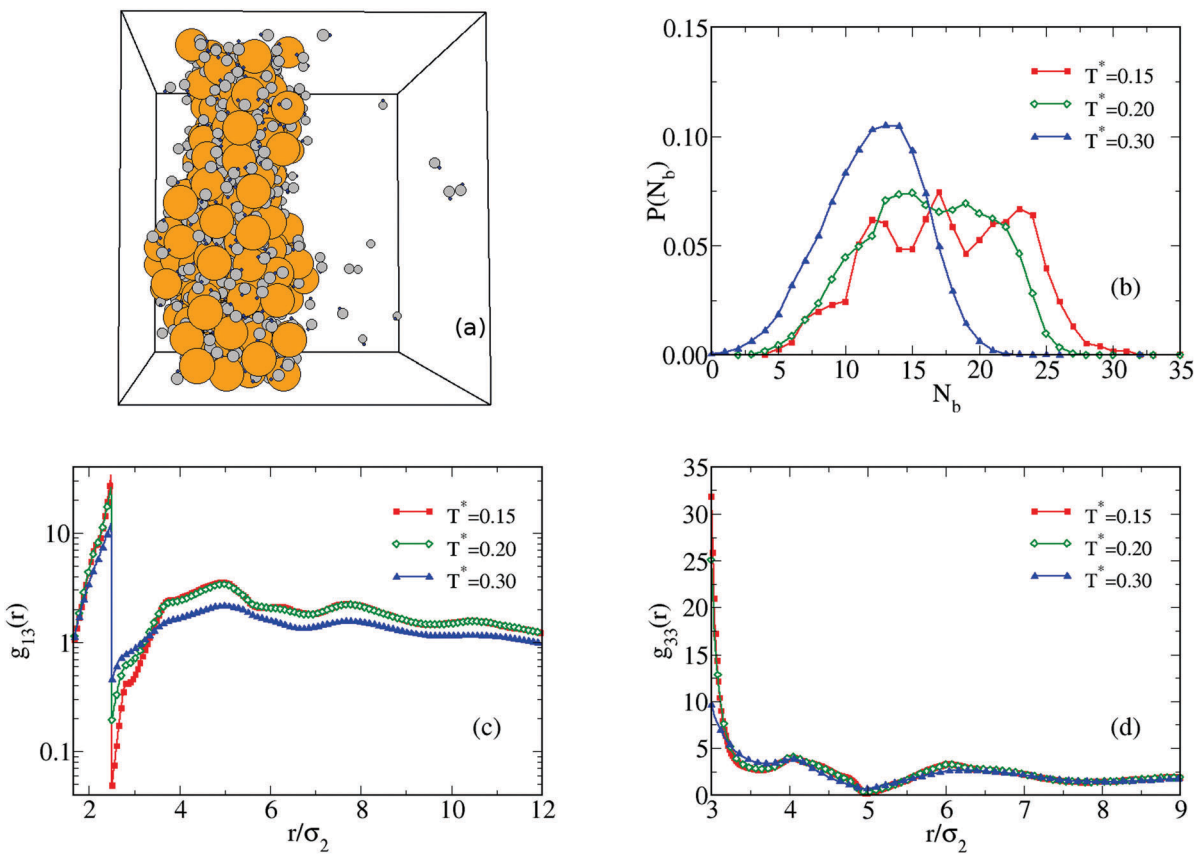

Fig. 5 Mixture of HJDs and guests with $\sigma_3 = 3\sigma_2$ and $\chi = 20\%$: (a) a microscopic configuration for $T^* = 0.30$; (b) $P(N_b)$ for various temperatures; (c) $g_{13}(r)$ (semilogarithmic scale) and (d) $g_{33}(r)$.

appear to be glued together with the HJD, forming a spatially extended slab-like structure, persisting also for lower temperatures. This arrangement is compatible with the coexistence of a guest-rich and a guest-poor phase, the latter being signaled by the few isolated HJDs visible in the snapshot. It is known that asymmetric binary hard-sphere mixtures are already close to a (metastable) demixing transition.[42,43] Specifically, smaller particles can induce phase separation in otherwise repulsive colloids, *via* depletion forces.[44] The presence of dimers in place of smaller spheres and the introduction of the 1–3 attraction are expected to stabilize such a transition. Additionally, since we investigate the regime of low temperatures, energetic effects also play an important role in promoting the phase separation. We observe that the peculiar planar shape of the condensate is made possible by the use of periodic boundaries in our simulations, an effect that is washed out in the bulk limit.[45,46] From the plot of $P(N_b)$ in Fig. 5b, we see that a guest sphere now binds a variable number of HJDs, mostly between 10 and 25, with no significant temperature dependence, as it could be expected for a liquid or an amorphous solid. This analysis is confirmed by the behavior of $g_{13}(r)$ and $g_{33}(r)$ in Fig. 5c and d, respectively; despite the fact that these functions refer to an inhomogeneous arrangement, their structure clearly reveals the existence of spatially extended correlations.

For $\sigma_3 = 3\sigma_2$ and intermediate concentrations, say $\chi = 10\%$, the $g_{33}(r)$ profile reported in Fig. 6a shows a marked oscillatory behavior characterized by several peaks, with some significant differences with respect to the $\chi = 20\%$ case of Fig. 5d. In fact, for $T^* \leq 0.20$ the main peak of $g_{33}(r)$ is now lower, but further peaks are more pronounced and the overall RDF appearance is typical of a system approaching solidification. The corresponding arrangement of the particles is reported in Fig. 6b: it appears that particles have all coalesced in a rather dense phase, leaving a rather large empty region in the box. We note that the peaks of $g_{33}(r)$ are sharper than those seen in Fig. 5d. The enhanced correlation between second and third neighbors for $\chi = 10\%$ reasonably results from a stronger effective attraction between guests, due to a comparatively larger number of gluing dimers. At variance with the planar shape found for $\chi = 20\%$ (Fig. 5a), we observe a cylindrical shape for $\chi = 10\%$, which is consistent with the overall smaller packing fraction of the system (see Table 1).[45,46]

As far as guest particles of smaller size are concerned, we have examined in more detail the case $\sigma_3 = \sigma_2/2$. Results for $\chi = 20\%$ and various temperatures are collected in Fig. 7. The short-distance profile of $g_{33}(r)$ in (a) documents a dramatic enhancement of the first-peak height, occurring for low temperatures; a secondary peak is also evident for $r/\sigma_2 \approx 0.8$. The latter is consistent with a linear 3–1–3 arrangement, whose length is indeed $\sigma_3/2 + \sigma_1 + \sigma_3/2 = 0.8$. Both features of $g_{33}(r)$ indicate the encapsulation of many guests together, in a global environment of dimers which also fill the interior of the capsules. Looking at the snapshot in Fig. 7b, we see that for $T^* = 0.30$ capsules have barely started to form around guests; indeed, the maximum of $P(N_b)$ is attained for $N_b = 0$ (see Fig. 7c), thus confirming that few bonds are formed under these conditions. Conversely, for $T^* = 0.10$ the attraction is strong enough to promote encapsulation, thus giving rise to small spherical clusters with a few numbers of touching guests bound to the surrounding HJDs (see the snapshot in Fig. 7d); the maximum of $P(N_b)$ has shifted towards higher values of N_b, with each guest preferentially binding six HJDs or more. For guest concentrations progressively lower than $\chi = 20\%$, encapsulation is found to become increasingly favored.

As far as the size ratio $\sigma_3 = \sigma_2$ is concerned, for $\chi = 20\%$ and $T^* = 0.30$ the system is essentially homogeneous (in particular, the maximum of $P(N_b)$ falls at $N_b = 0$, see Fig. 8a). Upon cooling the system down to $T^* = 0.10$, according to both panels in Fig. 8 spherical clusters eventually appear; similar to the case of $\sigma_3 = \sigma_2/2$, capsules are formed, even though the coating of dimers onto guests is less effective since capsules have large pores on their surface. A neat encapsulation is eventually obtained when $\chi = 10\%$ or less. A preliminary analysis of the internal structure of clusters shows that capsules containing a single guest are seldom observed, the average number of enclosed guests being 2.5 for $\chi = 10\%$ and 9.3 for $\chi = 20\%$. A more thorough investigation of the cluster structure from moderate to high values of χ is deferred to a forthcoming study.

The effectiveness of HJDs in forming capsules is summarized in Table 3, as a function of guest size, concentration, and temperature.

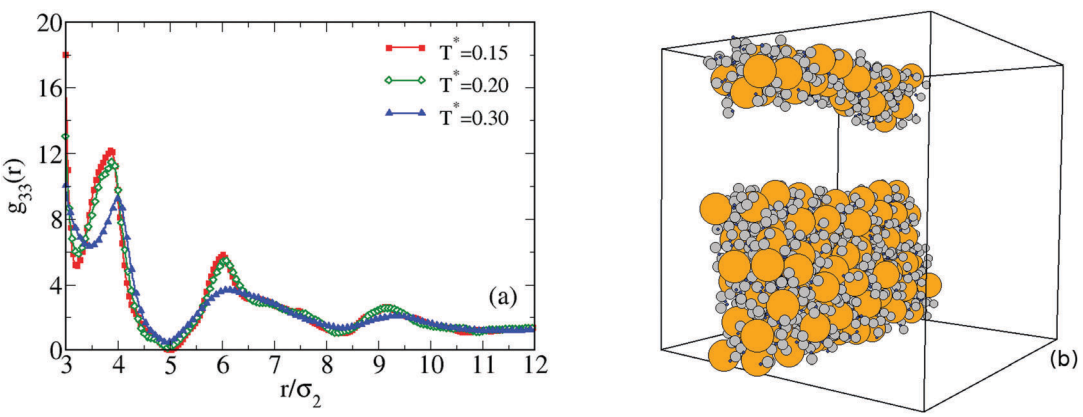

Fig. 6 Mixture of HJDs and guests with $\sigma_3 = 3\sigma_2$ and $\chi = 10\%$: (a) $g_{33}(r)$ for various temperatures and (b) a microscopic configuration for $T^* = 0.15$.

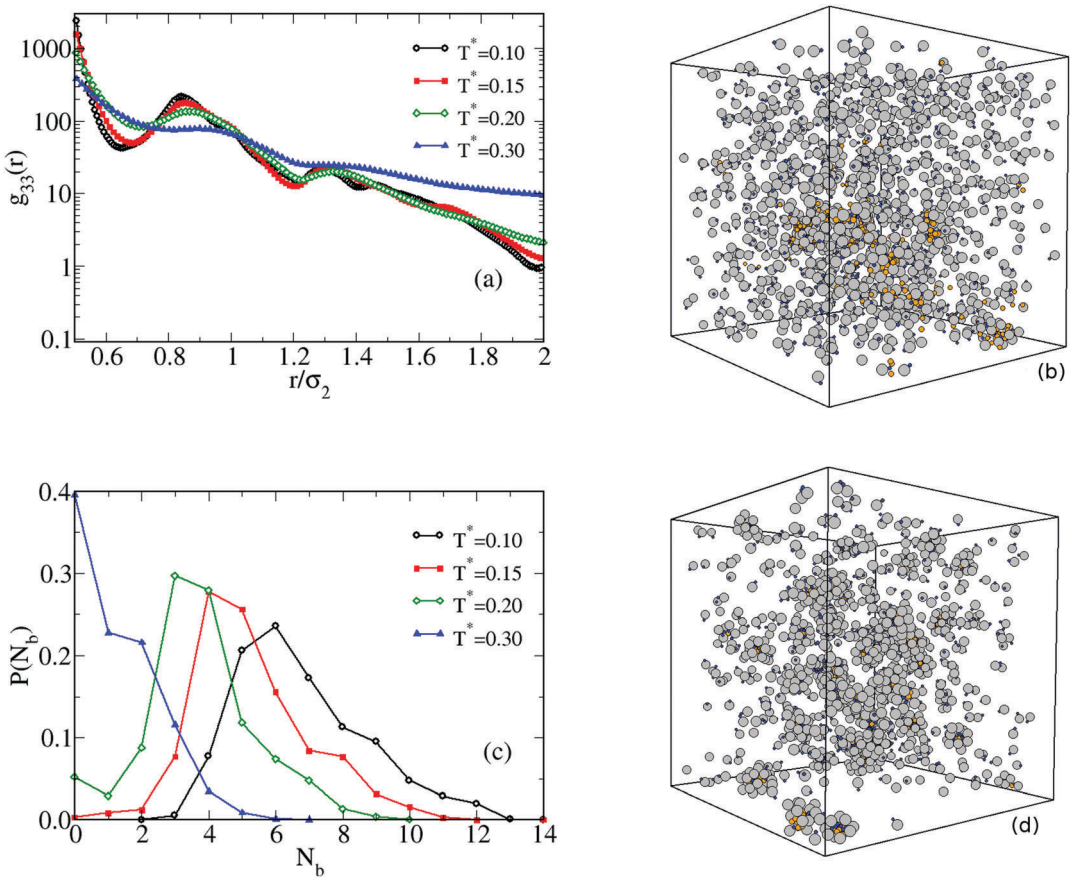

Fig. 7 Mixture of HJDs and guests with $\sigma_3 = \sigma_2/2$ and $\chi = 20\%$: (a) $g_{33}(r)$ (semilogarithmic scale); (b) a microscopic configuration for $T^* = 0.30$; (c) $P(N_b)$ for different temperatures; (d) a microscopic configuration for $T^* = 0.10$.

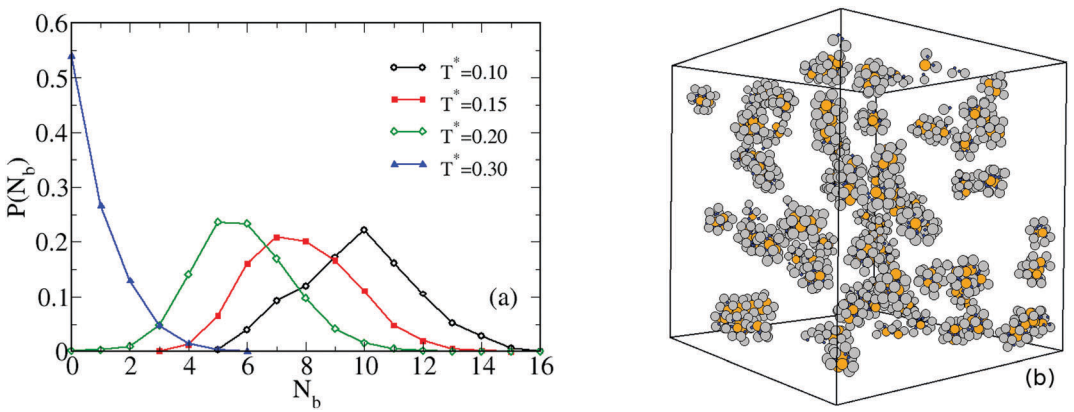

Fig. 8 Mixture of HJDs and guests with $\sigma_3 = \sigma_2$ and $\chi = 20\%$: (a) $P(N_b)$ for different temperatures and (b) a microscopic configuration for $T^* = 0.10$.

For $T^* = 0.10$ we see that small guests can easily be encapsulated for all concentrations, although the possibility to form single-guest capsules is difficult. As the guest size increases, progressively lower concentrations are required to achieve encapsulation, also because larger guest particles trivially need a higher number of dimers to be encapsulated. Specific conditions, as for instance large guest sizes and high concentrations, promote other interesting behaviors, such as phase separation between a guest-rich and a guest-poor phase. Looking at Table 3 we see that whenever phase separation can be avoided, capsules are always formed at sufficiently low temperature. For $T^* = 0.20$ only small guests are encapsulated, regardless of the concentration, whereas encapsulation is never achieved at the highest temperature investigated ($T^* = 0.30$). Moreover, in all cases where encapsulation eventually occurs, we have checked that the average number of bonds per guest is not less than one third of the maximum

Table 3 Summary of the encapsulation properties of the model mixture investigated in this work. Successful encapsulation is indicated by a checkmark

σ_3/σ_2	χ = 1%	χ = 10%	χ = 20%
T^* = 0.10			
0.5	✓	✓	✓
1.0	✓	✓	✓
3.0	✓	✗	✗
T^* = 0.20			
0.5	✓	✓	✓
1.0	✗	✗	✗
3.0	✗	✗	✗
T^* = 0.30			
0.5	✗	✗	✗
1.0	✗	✗	✗
3.0	✗	✗	✗

Table 4 Contact value of the guest–guest RDF as obtained from simulations at different temperatures

χ	$g_{hs}(\sigma^+)$ (eqn (2))	$g_{33}(\sigma^+)$, T^* = 0.30	$g_{33}(\sigma^+)$, T^* = 0.15
90%	1.0615	1.26	8.16
95%	1.0651	1.16	3.88

number allowed (see Table 2). The latter observation can tentatively be assumed as a hand-waving criterion for encapsulation, at least for the present system.

In agreement with a recent study of encapsulation by Janus ellipsoids,[35] we have found that small guests can more easily be encapsulated than larger ones; moreover, encapsulation is favored by increasing the strength of attraction between guests and ellipsoids, corresponding to either reducing temperature or guest concentration in our model.

We finally note that, in the limit of a vanishing number of dimers, our model reduces to a system of hard spheres. In order to investigate the approach to this limit we have simulated a binary mixture with $\sigma_3 = \sigma_2$ for χ = 90% and χ = 95%. In a fluid hard-sphere system, the value of the radial distribution function at contact, $g_{hs}(\sigma^+)$, is given by:[47]

$$g_{hs}(\sigma^+) = \frac{1 - \eta/2}{(1-\eta)^3}. \quad (2)$$

By substituting η with η_{guest} in eqn (2) we obtain the value of $g_{hs}(\sigma^+)$ for the corresponding hard-sphere system. By comparing this value with the contact value obtained from simulation, $g_{33}(\sigma^+)$, we have an idea of the effect of a relatively small number of dimers on the local structure of guests. The results for this comparison are reported in Table 4: as is clear, even for very high concentrations of guests, $g_{33}(\sigma^+)$ is still far from the hard-sphere value when T^* = 0.15. Conversely, for T^* = 0.30 the deviation is quite small.

IV Conclusions and perspectives

We have investigated the spontaneous formation of capsules (*i.e.* through self-assembly) in a dilute mixture of heteronuclear Janus dimers and guest spheres. In this model, both dimers and guests are taken to be hard particles; additionally, the smaller sphere of a dimer interacts with a guest particle through a square-well attraction. We have carried out standard Monte Carlo simulations in the canonical ensemble to characterize the fluid structure and to study the formation of capsules around guests. To this aim, we have varied both the guest size and concentration, finding that small values of both properties are indeed able to promote the formation of capsules enclosing one or few guests. Moving to higher values of the guest size other phase scenarios become possible, including the formation of a rather compact (liquid or solid) phase where dimers and guests are tied together. In this respect, the possibility to segregate guests may represent another useful approach for their separation and extraction from the solution, even in the absence of neat encapsulation. Upon reducing the concentration of large guests down to one percent, capsules are recovered again, at least provided that the temperature is low enough.

The coating of a target molecule with colloidal particles in a solvent is an issue of major interest in a wide range of fields, such as food nanotechnologies and drug delivery. In this regard, we consider the present study as a preliminary step to more extended investigations of the encapsulation process. In the near future we plan to formulate a quantitative criterion for successful encapsulation based on a precise identification of guest clusters within the simulation. Possible developments of our model might envisage the inclusion of the solvent and a more realistic description of guest particles and interactions, with the idea to study encapsulation and ensuing extraction of noble components from complex colloidal solutions like, for instance, beta-lactoglobulins from whey milk or DNA fragments from biological environments.

Acknowledgements

We thank Prof. Giacomo Dugo for useful comments and ongoing collaboration. We also thank Prof. Francesco Sciortino for helpful suggestions and discussions. Support from the PRIN-MIUR 2010-2011 project is also gratefully acknowledged.

References

1 R. Haag, *Angew. Chem., Int. Ed.*, 2004, **43**, 278.
2 L. Zhang, *et al.*, *ACS Nano*, 2008, **2**, 1696.
3 L. Sanguansri and M. A. Augustin, in *Microencapsulation in Functional Food Product Development*, ed. J. Smith and E. Charter, Wiley-Blackwell, 2010.
4 S. D. Perrault and W. M. Shih, *ACS Nano*, 2014, **8**, 5132.
5 A. H. E. Machado, D. Lundberg, A. J. Ribeiro, F. J. Veiga, M. G. Miguel, B. Lindman and U. Olsson, *Langmuir*, 2013, **29**, 15926.
6 E. Haladjova, S. Rangelov, C. B. Tsvetanov and S. Pispas, *Soft Matter*, 2012, **8**, 2884.
7 A. Madene, M. Jacquot, J. Scher and S. Desobry, *Int. J. Food Sci. Technol.*, 2006, **41**, 1.

8 A. K. Anal and H. Singh, *Trends Food Sci. Technol.*, 2007, **18**, 240.
9 M. A. Augustin and Y. Hemar, *Chem. Soc. Rev.*, 2008, **38**, 902.
10 Q. Tang and A. R. Denton, *Phys. Chem. Chem. Phys.*, 2015, **17**, 11070.
11 Y. Hennequin, N. Pannacci, C. P. de Torres, G. Tetradis-Meris, S. Chapuliot, E. Bouchaud and P. Tabeling, *Langmuir*, 2009, **25**, 7857.
12 L. M. Dominak and C. D. Keating, *Langmuir*, 2007, **23**, 7148.
13 A. Rösler, G. W. Vandermeulen and H. A. Klok, *Adv. Drug Delivery Rev.*, 2001, **53**, 95.
14 R. Malik, J. Genzer and C. K. Hall, *Langmuir*, 2015, **31**, 3518.
15 T. S. Skelhon, Y. Chen and S. A. F. Bon, *Soft Matter*, 2014, **10**, 7730.
16 D. J. Kraft, R. Ni, F. Smallenburg, M. Hermes, K. Yoon, D. Weitz, A. van Blaaderen, J. Groenewold, M. Dijkstra and W. Kegel, *Proc. Natl. Acad. Sci. U. S. A.*, 2012, **109**, 10787.
17 D. Nagao, K. Goto, H. Ishii and M. Konno, *Langmuir*, 2011, **27**, 13302.
18 K. Yoon, D. Lee, J. W. Kim, J. Kim and D. A. Weitz, *Chem. Commun.*, 2012, **48**, 9056.
19 I. D. Hosein and C. M. Liddell, *Langmuir*, 2007, **23**, 10479.
20 G. A. Chapela, F. del Río and J. Alejandre, *J. Chem. Phys.*, 2011, **134**, 224105.
21 P. Ilg and E. Del Gado, *Soft Matter*, 2011, **7**, 163.
22 S. H. Chong, A. J. Moreno, F. Sciortino and W. Kob, *Phys. Rev. Lett.*, 2005, **94**, 215701.
23 G. Munaò, D. Costa, A. Giacometti, C. Caccamo and F. Sciortino, *Phys. Chem. Chem. Phys.*, 2013, **15**, 20590.
24 G. Munaò, P. O'Toole, T. S. Hudson, D. Costa, C. Caccamo, A. Giacometti and F. Sciortino, *Soft Matter*, 2014, **10**, 5269.
25 F. Tu, B. J. Park and D. Lee, *Langmuir*, 2013, **29**, 12679.
26 B. J. Park and D. Lee, *ACS Nano*, 2012, **6**, 782.
27 L. Hong, A. Cacciuto, E. Luijten and S. Granick, *Langmuir*, 2008, **24**, 621–625.
28 C.-H. Chen, R. K. Shah, A. R. Abate and D. A. Weitz, *Langmuir*, 2009, **25**, 4320–4323.
29 Q. Chen, J. Yan, J. Zhang, S. C. Bae and S. Granick, *Langmuir*, 2012, **28**, 1355.
30 F. Sciortino, A. Giacometti and G. Pastore, *Phys. Rev. Lett.*, 2009, **103**, 237801.
31 B. S. Jiang, Q. Chen, M. Tripathy, E. Luijten, K. Schweizer and S. Granick, *Adv. Mater.*, 2010, **22**, 1060.
32 G. Rosenthal, K. E. Gubbins and S. H. Klapp, *J. Chem. Phys.*, 2012, **136**, 174901.
33 W. Li, Y. Liu, G. Brett and J. D. Gunton, *Soft Matter*, 2012, **8**, 6027.
34 D. Ruth, J. D. Gunton, J. M. Rickman and W. Li, *J. Chem. Phys.*, 2014, **141**, 214903.
35 W. Li, D. Ruth, J. D. Gunton and J. M. Rickman, *J. Chem. Phys.*, 2015, **142**, 244705.
36 G. Munaò, P. O. Toole, T. S. Hudson, D. Costa, C. Caccamo, F. Sciortino and A. Giacometti, *J. Phys.: Condens. Matter*, 2015, **37**, 234101.
37 G. Avvisati, T. Vissers and M. Dijkstra, *J. Chem. Phys.*, 2015, **142**, 084905.
38 J. R. Bordin, L. B. Krott and M. C. Barbosa, *Langmuir*, 2015, **31**, 8577.
39 S. Prestipino, M. Ferrario and P. V. Giaquinta, *Physica A*, 1992, **187**, 456.
40 S. Prestipino, M. Ferrario and P. V. Giaquinta, *Physica A*, 1993, **201**, 649.
41 S. Prestipino and P. V. Giaquinta, *J. Stat. Phys.*, 1993, **75**, 1093.
42 M. Dijkstra, R. van Roij and R. Evans, *Phys. Rev. Lett.*, 1998, **81**, 2268.
43 M. Dijkstra, R. van Roij and R. Evans, *Phys. Rev. E: Stat. Phys., Plasmas, Fluids, Relat. Interdiscip. Top.*, 1999, **59**, 5744.
44 A. A. Louis, E. Allahyarov, H. Lowen and R. Roth, *Phys. Rev. E: Stat., Nonlinear, Soft Matter Phys.*, 2002, **65**, 061407.
45 M. C. Abramo, C. Caccamo, D. Costa, P. V. Giaquinta, G. Malescio, G. Munaò and S. Prestipino, *J. Chem. Phys.*, 2015, **142**, 214502.
46 S. Prestipino, C. Caccamo, D. Costa, G. Malescio and G. Munaò, *Phys. Rev. E: Stat., Nonlinear, Soft Matter Phys.*, 2015, **92**, 022141.
47 N. F. Carnahan and K. E. Starling, *J. Chem. Phys.*, 1969, **51**, 635.